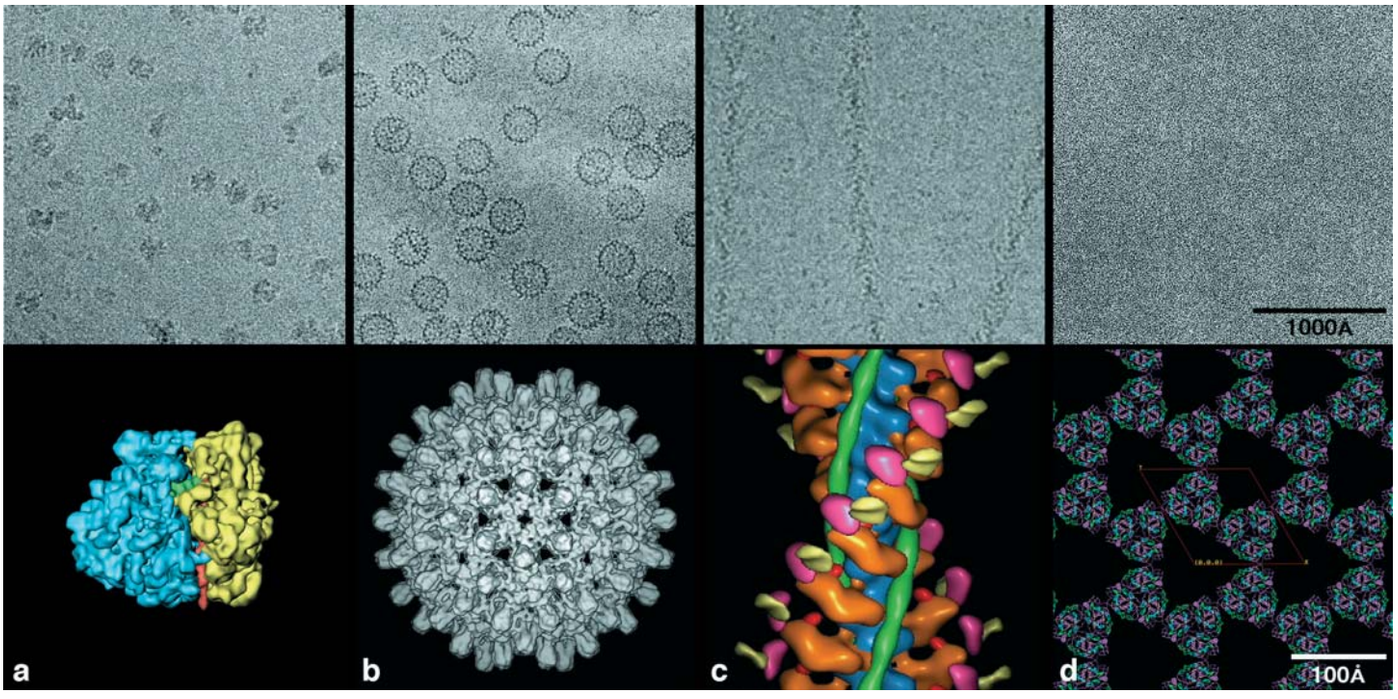

Fig. 19.6.5.1. Examples of macromolecules studied by cryo EM and 3D image reconstruction and the resulting 3D structures (bottom row) after cryo EM analysis. All micrographs (top row) are displayed at ∼170 000× magnification and all models at ∼1 200 000× magnification. (*a*) A single particle without symmetry. The micrograph shows 70S *E. coli* ribosomes complexed with mRNA and fMet-tRNA. The surface-shaded density map, made by averaging 73 000 ribosome images from 287 micrographs, has a resolution of 11.5 Å. The 50S and 30S subunits and the tRNA are coloured blue, yellow and green, respectively. The identity of many of the protein and RNA components is known and some RNA double helices are clearly recognizable by their major and minor grooves (*e.g.* helix 44 is shown in red). Courtesy of J. Frank (SUNY, Albany), using unpublished data from I. Gabashvili, R. Agrawal, C. Spahn, R. Grassucci, J. Frank & P. Penczek. (*b*) A single particle with symmetry. The micrograph shows hepatitis B virus cores. The 3D reconstruction, at a resolution of 7.4 Å, was computed from 6384 particle images taken from 34 micrographs. From Böttcher, Wynne & Crowther (1997). (*c*) A helical filament. The micrograph shows actin filaments decorated with myosin S1 heads containing the essential light chain. The 3D reconstruction, at a resolution of 30–35 Å, is a composite in which the differently coloured parts are derived from a series of difference maps that were superimposed on F-actin. The components include: F-actin (blue), myosin heavy-chain motor domain (orange), essential light chain (purple), regulatory light chain (white), tropomyosin (green) and myosin motor domain N-terminal beta-barrel (red). Courtesy of A. Lin, M. Whittaker & R. Milligan (Scripps Research Institute, La Jolla). (*d*) A 2D crystal: light-harvesting complex LHCII at 3.4 Å resolution. The model shows the protein backbone and the arrangement of chromophores in a number of trimeric subunits in the crystal lattice. In this example, image contrast is too low to see any hint of the structure without image processing (see also Fig. 19.6.4.2). Courtesy of W. Kühlbrandt (Max-Planck-Institute for Biophysics, Frankfurt).

(Pebay-Peyroula *et al.*, 1997; Essen *et al.*, 1998; Luecke *et al.*, 1998). (2) Density maps of the 50S ribosomal subunits from two species obtained by cryo EM (Frank *et al.*, 1995; Ban *et al.*, 1998) were used to help solve the X-ray crystal structure of the *Haloarcula marismortui* 50S subunit (Ban *et al.*, 1998).

19.6.5. Recent trends

The new generation of intermediate-voltage (∼300 kV) FEG microscopes becoming available is now making it much easier to obtain higher-resolution images which, by use of larger defocus values, have good image contrast at both very low and very high resolution. The greater contrast at low resolution greatly facilitates particle-alignment procedures, and the increased contrast resulting from the high-coherence illumination helps to increase the signal-to-noise ratio for the structure at high resolution. Cold stages are constantly being improved, with several liquid-helium stages now in operation (*e.g.* Fujiyoshi *et al.*, 1991; Zemlin *et al.*, 1996). Two of these are commercially available from JEOL and FEI/Philips/Gatan. The microscope vacuums are improving so that the bugbear of ice contamination in the microscope, which prevents prolonged work on the same grid, is likely to disappear soon. The improved drift and vibration performance of the cold stage means longer (and therefore more coherently illuminated) exposures at higher resolution can be recorded more easily. Hopefully, the first atomic structure of a single-particle macromolecular assembly solved by electron microscopy will soon become a reality.

Finally, three additional likely trends include: (1) increased automation, including the recording of micrographs, and the use of spot-scan procedures in remote microscope operation (Kisseberth *et al.*, 1997; Hadida-Hassan *et al.*, 1999) and in every aspect of image processing; (2) production of better electronic cameras (*e.g.* CCD or pixel detectors); and (3) increased use of dose-fractionated, tomographic tilt series to extend EM studies to the domain of larger supramolecular and cellular structures (McEwen *et al.*, 1995; Baumeister *et al.*, 1999).

Acknowledgements

We are greatly indebted to all our colleagues at Purdue and Cambridge for their insightful comments and suggestions, to B. Böttcher, R. Crowther, J. Frank, W. Kühlbrandt and R. Milligan for supplying images used in Fig. 19.6.5.1, which gives some examples of the best work done recently, and J. Brightwell for editorial assistance. TSB was supported in part by grant GM33050 from the National Institutes of Health.

references